Dominance of Milnor Attractors and Noise-Induced Selection in a Multiattractor System

Kunihiko Kaneko

Department of Pure and Applied Sciences, College of Arts and Sciences, University of Tokyo,
Komaba, Meguro-ku, Tokyo 153, Japan
(Received 27 September 1996)

In a multiattractor state of a globally coupled dynamical system, stability of the attractors is studied by recording the return rates to themselves after perturbations. Besides the basin volume, attractors are characterized by strength, defined as the threshold perturbation for the full return rate. It is observed that Milnor attractors with a vanishing strength are dominant in the partially ordered phase. Attractions to weak attractors are found to be often enhanced with the addition of a noise, selectively for its amplitude.   [S0031-9007(97)02844-5]

PACS numbers: 05.45.+b, 05.40.+j

Multiattractor systems are important in physical, chemical, biological, and engineering problems. Although the (fractal) basin structures [1] have been studied in a low-dimensional system, dynamics and the phase structure are not fully understood for a system with large degrees of freedoms, where *static* structures of rugged landscape have been mostly studied. Since performing a direct "anatomy" of the phase space structure is difficult there, we introduce new quantifiers to characterize the stability (strength) of attractors and connections among them, besides the basin volume.

Two main discoveries are reported: The first one states that the probability of initial points to fall onto "fragile" (i.e., "Milnor") attractors [2,3] is rather high within some region between ordered and turbulent phases. Here the Milnor attractor is defined as a state that some perturbations of arbitrary small size can kick the orbit out of it although a finite measure of initial points is attracted to it. Since such an asymptotically unstable attractor is often believed to be a rather exceptional state, the dominance of such attractors is a remarkable observation.

The second is the noise-induced selection of attractors: By adding a noise for a while, the ratio of the orbits to fall into weak attractors is enhanced, in some parameter regime, in contrast with our intuition. Different attractors are successively selected specific to the noise strength, which may reflect on the complex basin structures. The relevance of these results to neural dynamics is also discussed.

As an example of a high-dimensional dynamical system with potentially many attractors, we adopt the globally coupled map (GCM) [4] given by

$$x_{n+1}(i) = (1 - \epsilon)f(x_n(i)) + \frac{\epsilon}{N} \sum_{j=1}^{N} f(x_n(j)), \quad (1)$$

where n is a discrete time step and i is the index for elements ($i = 1, 2, \ldots, N$ = system size). Here we choose the logistic map $f(x) = 1 - ax^2$ ($-1 < x < 1$) as the local element in Eq. (1), as it has been investigated extensively as a standard model for a high-dimensional dy-

namical system. In the model, attractors can be coded by clustering, the partition of elements into mutually synchronized clusters, i.e., a set of elements with $x_n(i) = x_n(j)$ [4]. Attractors in this GCM are classified by the number of synchronized clusters k and the number of elements for each cluster N_j. Each attractor is coded by the clustering condition $[N_1(\geq), N_2(\geq), \ldots, (\geq)N_k]$ (also called its partition). Because of symmetry, there are at least $\frac{N!}{\prod_{i=1}^{k} N_i!} \prod_{\text{sets of } N_i=N_j} \frac{1}{m_\ell!}$ attractors for each clustering condition, where m_ℓ is the number of clusters with the same value of N_j [5].

With an increase of the nonlinear parameter a or a decrease of the coupling ϵ, the following phases are known to appear successively [4] after the collapse of a completely synchronized state. (i) *Ordered phase*: all attractors consist of a few [$k = o(N)$] clusters. (ii) *Partially ordered (PO) phase*: attractors with a variety of clusterings coexist, most of them having many clusters [$k = O(N)$]. (iii) *Turbulent phase*: elements are completely desynchronized, and all attractors have N clusters. In the first two phases, there exist a variety of attractors depending on the partition [6]. In the present Letter, we study the multiattractor structure for these two phases, fixing $\epsilon = 0.1$ and varying a.

To study the stability of an attractor against perturbation, we introduce the return probability $P(\sigma)$, defined as follows: Take an orbit point $\{x(i)\}$ of an attractor in an N-dimensional phase space, and perturb the point to $x(i) + \frac{\sigma}{2}\text{rnd}_i$, where rnd_i is a random number taken from $[-1, 1]$, uncorrelated for all elements i. Check if this perturbed point returns to the original attractor via the deterministic dynamics (1). By sampling over random perturbations and orbit positions, the return probability $P(\sigma)$ is defined as (No. of returns)/(No. of perturbation trials) (see Fig. 1). As a simple index for robustness of an attractor, it is useful to define σ_c as the largest σ such that $P(\sigma) = 1$, and σ_m the smallest σ s.t. $P(\sigma) < 0.5$. These indices measure what we call the *strength* of an attractor.

The strength σ_c gives a minimum distance between the orbit of an attractor and its basin boundary. Note that
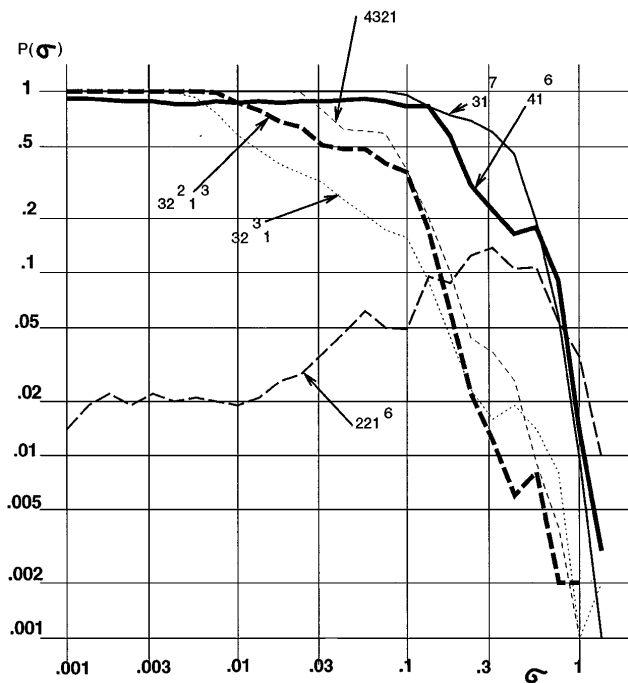
FIG. 1. Example of $P(\sigma)$ for $a = 1.61$ and $N = 10$. For all the figures, we take 10^4 initial conditions randomly chosen over $[-1, 1]$ for each value of parameter a. $P(\sigma)$ is estimated by sampling over 10^3 random perturbations for each σ. Throughout this Letter we often abbreviate an attractor's clustering condition, using $32^2 1^3$ in place of $[3, 2, 2, 1, 1, 1]$, for example.

σ_c can be small, even if the basin volume is large, if the attractor is located near the basin boundary. We have plotted σ_c versus basin volume, which is measured as the probability that an orbit with a randomly chosen initial condition falls onto the attractor. Roughly speaking, the plot shows the existence of three types of attractors. One type keeps some relationship between σ_c and basin volume [7], while the other two types do not. One of the latter two types is a Milnor attractor [2,3], having $\sigma_c = 0$ with a finite (large) basin measure, and the other is a strong attractor with a relatively small basin volume.

The Milnor attractor has been recently studied as a riddled basin attractor [3,8]. For a coupled system, attraction to a (partially) synchronized state is found that has a riddled basin [9] and an instability in any neighborhood of an attractor [3,10]. As has been expected [3,8], all of the Milnor attractors we have found are chaotic.

There are two types of Milnor attractors; one has $\sigma_m = 0$ (e.g., $[2^2, 1^6]$ of Fig. 1), where most tiny perturbations can kick the orbit out of the "attractor." Indeed, we have seen that iterations of (1) with any finite precision (i.e., by a digital computer) can lead to such an attractor due to artificial synchronization of $x_n(i)$ [10]. For the other type, $P(\sigma \to 0)$ is close to 1 (e.g., $[4, 1^6]$ of Fig. 1). It is a fragile attractor, in the sense that some tiny perturbation kicks an orbit out of it. It should be noted that such fragile

attractors can have a large basin measure. For both types, $P(\sigma)$ sometimes increases with the increase of σ (see $[2^2, 1^6]$ of Fig. 1).

In Fig. 2, we have plotted the distribution of strength σ_c versus the change of a. Note the decrease of strength starting around $a \approx 1.56$, and the dominance of weak attractors at $a = (\sim 1.67 - 1.68)$. The averages of basin volume and attractor strengths (over random initial configurations) are plotted in Fig. 3. The results are summarized as follows:

(I) $a \lesssim 1.61$ [11] (ordered phase): Strong attractors ($\sigma_c > 0.1$) with 2 or 3 clusters have rather large basin volumes. Fragile attractors do not exist, or have a very small basin volume (1%) if they do exist.

(II) $1.61 \lesssim a \lesssim 1.65$ [complex ordered (CO) regime]: There are a variety of attractors with different partitions, although the number of clusters is not huge [i.e., $o(N)$ for large N]. Fragile attractors with a large basin volume appear, as well as strong attractors with a small number of clusters.

(III) $1.65 \lesssim a \lesssim 1.68$ (PO phase): The number of clusters is typically large $[O(N)]$, while the basin volume for each attractor is much larger than the case (II). For example, at $a = 1.66$ and $N = 10$, the basin volume of the attractors with $[2^2, 1^6]$ occupies 60% of the total, while that of $[1^{10}]$ has 30%. Remarkably, these attractors are fragile ($\sigma_c < 10^{-4}$). This dominance of fragile attractors is preserved as N is increased, although the region of the PO phase is slightly shifted.

(IV) At $a \gtrsim 1.69$, a single desynchronized attractor exists.
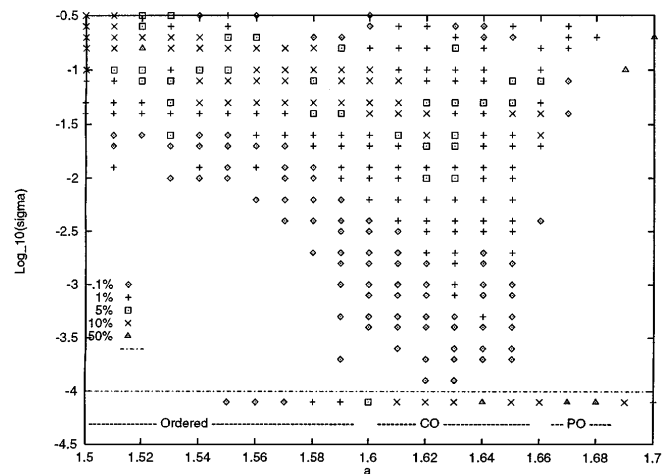
FIG. 2. Dependence of σ_c on the parameter a, for $N = 50$. By measuring σ_c for attractors settled in from 10^4 random initial conditions, a histogram of $\log_{10} \sigma_c$ is constructed with a bin size 0.1. The number of initial conditions leading to $\log_{10} \sigma_c$ within the bin is plotted as different marks: $\triangle$ ($>$50%), $\bigcirc$ ($>$10%), $\square$ ($>$5%), $+$ ($>$1%), and $\diamond$ ($>$0.1%). For all figures we have estimated σ_c from 100 possible perturbations: σ_c is regarded to be larger than the σ value adopted in the run, as long as all of the 100 trials result in the return to the original attractor, while σ is changed successively with 20% from 10^{-4}. The points at $\sigma_c < 10^{-4}$ just represent that $\sigma_c < 10^{-4}$.
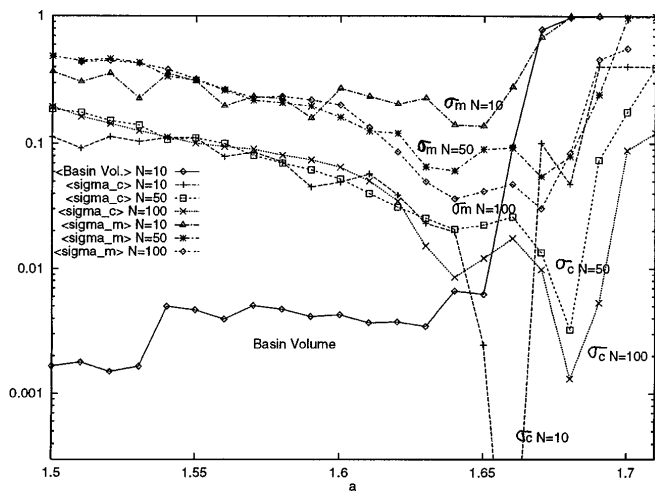
FIG. 3. Averages of strength $\langle \sigma_c \rangle$, $\langle \sigma_m \rangle$, and basin volume are plotted as a function of a. The basin volume of each attractor is estimated as the rate of initial points leading to the attractor, divided by the degeneracy [5]. The average is taken over 10^4 random initial conditions as in Fig. 1. σ_m is estimated from $P(\sigma)$, measured by changing σ as $10^{-4+j/4}$ for ($j = 0, 1, \ldots, 16$). For $N = 50$ and $N = 100$, we have made only 100 possible perturbations instead of 10^3.

With the increase of N, σ_c for attractors with a proportional partition (e.g., $[6, 4]$ for $N = 10$ versus $[60, 40]$ for $N = 100$) remains unchanged, while $\sigma_m - \sigma_c$ is decreased. The latter is due to the increase of the dimension of the path out of the attractor, since the decay of $P(\sigma)$ for $\sigma > \sigma_c$ reflects on the volume of the path. In Fig. 3, the decrease of $\langle \sigma_m \rangle$ with N is confirmed at the CO and PO phases (where $\langle \sigma_c \rangle$ is small). At the PO phase, the dominance of weak attractors is prominent for large N, as is seen in the decrease of $\langle \sigma_c \rangle$ with N.

We have also studied the transition matrix among attractors that gives the rate of transition from one attractor to another when the former is perturbed by a noise. In general, weak attractors are connected to a variety of attractors. Small perturbations to such attractors make the orbit fall into a variety of different attractors.

Coexistence of attractors with different degrees of stability makes us expect that noise is relevant to the choice of the attractor the GCM settles in. One might expect that noise usually leads the system to choose to settle in strong attractors. We have simulated the model (1) for a fixed number of steps with white uncorrelated noise added to each element and then checked which attractor is selected after the noise is turned off [12]. $\langle \sigma_c \rangle$ is plotted in Fig. 4 with the change of the noise strength δ. In contrast with the PO phase, relatively weaker attractors are selected in the CO phase, contrary to our expectation [13]. This is possibly because more transient orbits are attracted to some of the weak attractors due to higher connectivity with other attractors in the transition matrix.

A remarkable feature is its sensitivity in the choice of attractors depending on the strength of the noise added.
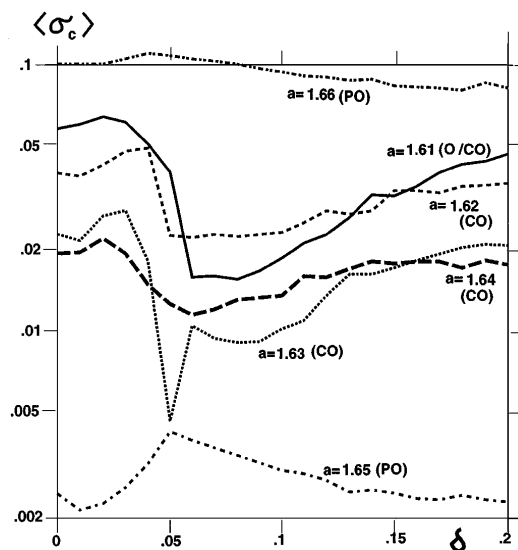
FIG. 4. Change of average strength $\langle \sigma_c \rangle$ against the noise strength. Starting from random initial conditions, we have computed the model (1) with an additional noise term $(\delta/2) \times \mathrm{rnd}_n(i)$ over 10^4 steps, and checked which attractor is selected after the noise is turned off. N is 10, although the same behaviors are seen for larger N (e.g., 50). Note that the parameter for the top line is near the turbulent phase, and strong attractors have a larger basin volume than Milnor ones, leading to large $\langle \sigma_c \rangle$. Still, the escape from remaining Milnor attractors by noise leads to the slight increase of the strength around $\delta \approx 0.04$.

At some noise strengths, the basin volume of some attractors is enhanced rather sharply. In Fig. 5, we have plotted the number of initial points falling onto attractors versus the noise strength applied during transient steps. There are successive enhancements of attraction rates to some attractors. This stochastic amplification is a novel noise effect, which is due to complex connection paths among attractors. The peak around $\delta \approx 0.04$ for the attractor $[3, 1^7]$ in Fig. 5, for example, is due to the gap between the thresholds of noise strengths leading to the transitions $[3, 1^7] \rightarrow$ others and the reverse ones.

In high-dimensional dynamical systems, chaotic itinerancy (CI) among several ordered states is often observed [4,14,15]. For Milnor attractors that lose their stability $[P(0) < 1]$ but keep their attraction for large σ, the total system dynamics can be constructed as the successive alternations between attraction to and escape from them. Hence CI is understood as the connection among many Milnor attractors.

In the present Letter, we have proposed that Milnor attractors dominate the basin volume in the PO phase. Although our results are based on the GCM (1), it is expected that the same qualitative behavior is observed in high-dimensional dynamical systems, including coupled differential equation systems [16]. It is also interesting to note the relevance of the present results to neural dynamics. Freeman has found a chaotic attractor corresponding
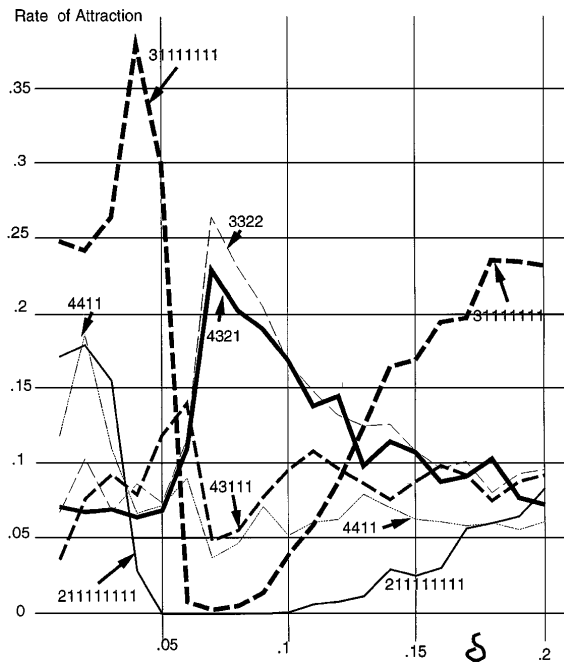
FIG. 5. Rates of attraction to some attractors with the change of transient noise, for $N = 10$. Computations are carried out in the same manner as Fig. 4. Only six attractors with larger attraction rates are plotted.

to a searching state for memories [17]. The weak attractors in the CO or PO phases provide a candidate for such a searching state, because they are connected to a variety of stronger attractors, which, in this interpretation, would play the role of memorized states in Freeman's work.

[1] C. Grebogi, E. Ott, and J. A. Yorke, Phys. Rev. Lett. **50**, 935 (1983); Physica (Amsterdam) **24D**, 243 (1987); S. Takesue and K. Kaneko, Prog. Theor. Phys. **71**, 35 (1984).

[2] J. Milnor, Commun. Math. Phys. **99**, 177 (1985); **102**, 517 (1985).

[3] P. Ashwin, J. Buescu, and I. Stuart, Nonlinearity **9**, 703 (1996).

[4] K. Kaneko, Physica (Amsterdam) **41D**, 38 (1990); **54D**, 5 (1991).

[5] For example, the latter factor for the clustering $[2, 2, 2, 1, 1, 1, 1]$ is $1/(3! \, 4!)$. This estimation is based on two assumptions: first, that clusters with the same number of elements are indistinguishable due to symmetry and, second, that all attractors with the same partition are unique. This latter assumption is not exactly true, but degeneracy is rather rare in practice.

[6] Correspondence of the PO phase with a spin glass has been studied in K. Kaneko, J. Phys. A **24**, 2107 (1991); A. Crisanti, M. Falcioni, and A. Vulpiani, Phys. Rev. Lett. **76**, 612 (1996).

[7] The plots scatter around the linear relationship between the strength and basin volume. As a schematic example, assume that the basin is given by a hyperellipsoid with the radii $r_1(\leq), r_2(\leq), \ldots, (\leq)r_N$, and the attractor is localized at the center of it. Then the strength σ_c is given by r_1. If r_1 sensitively depends on parameters or attractors (e.g., as in the case near the crisis) and $r_j \, (j > 1)$ remains larger, we could estimate basin volume $\propto \sigma_c$.

[8] J. C. Sommerer and E. Ott, Nature (London) **365**, 138 (1993); E. Ott *et al.,* Phys. Rev. Lett. **71**, 4134 (1993).

[9] Y-C. Lai and R. L. Winslow, Physica (Amsterdam) **74D**, 353 (1994); Y-C. Lai and C. Grebogi, Phys. Rev. E **53**, 1371 (1996).

[10] K. Kaneko, Physica (Amsterdam) **77D**, 456 (1994), where such a state is called a pseudoattractor.

[11] The boundary of the phases shifts with N if N is not large enough (e.g., $\lesssim 50$). For example, the region of the PO phase shifts upwards with an increase of N.

[12] Instead of the switching noise, it may be more natural to study a system in which a noise is always added, but $\langle \sigma_c \rangle$ cannot be measured then. Roughly speaking, our attraction ratio estimates the residence time at the neighborhood of each attractor for the noisy system. On the other hand, the switching of inputs (noise) is relevant to a neural system discussed later.

[13] For large δ, the memory of previous attractors is lost, which essentially leads to random sampling of initial configurations. Hence the average strength comes back to the level of the noiseless case, for large δ.

[14] I. Tsuda, World Futures **32**, 167 (1991); Neural Networks **5**, 313 (1992).

[15] K. Ikeda *et al.,* Prog. Theor. Phys. Suppl. **99**, 295 (1989).

[16] D. Dominguez and H. A. Cerdeira, Phys. Rev. Lett. **71**, 3359 (1993).

[17] W. Freeman and C. A. Skarda, Brain Res. Rev. **10**, 147 (1985).